

# **SANDIA REPORT**

SAND2009-7941

Unlimited Release

Printed January 2010

## **Local Magnitudes of Small Contained Explosions**

Eric P. Chael

Prepared by  
Sandia National Laboratories  
Albuquerque, New Mexico 87185 and Livermore, California 94550

Sandia is a multiprogram laboratory operated by Sandia Corporation, a Lockheed Martin Company, for the United States Department of Energy's National Nuclear Security Administration under Contract DE-AC04-94AL85000.

Approved for public release; further dissemination unlimited.



Issued by Sandia National Laboratories, operated for the United States Department of Energy by Sandia Corporation.

**NOTICE:** This report was prepared as an account of work sponsored by an agency of the United States Government. Neither the United States Government, nor any agency thereof, nor any of their employees, nor any of their contractors, subcontractors, or their employees, make any warranty, express or implied, or assume any legal liability or responsibility for the accuracy, completeness, or usefulness of any information, apparatus, product, or process disclosed, or represent that its use would not infringe privately owned rights. Reference herein to any specific commercial product, process, or service by trade name, trademark, manufacturer, or otherwise, does not necessarily constitute or imply its endorsement, recommendation, or favoring by the United States Government, any agency thereof, or any of their contractors or subcontractors. The views and opinions expressed herein do not necessarily state or reflect those of the United States Government, any agency thereof, or any of their contractors.

Printed in the United States of America. This report has been reproduced directly from the best available copy.

Available to DOE and DOE contractors from

U.S. Department of Energy  
Office of Scientific and Technical Information  
P.O. Box 62  
Oak Ridge, TN 37831

Telephone: (865) 576-8401  
Facsimile: (865) 576-5728  
E-Mail: [reports@adonis.osti.gov](mailto:reports@adonis.osti.gov)  
Online ordering: <http://www.osti.gov/bridge>

Available to the public from

U.S. Department of Commerce  
National Technical Information Service  
5285 Port Royal Rd.  
Springfield, VA 22161

Telephone: (800) 553-6847  
Facsimile: (703) 605-6900  
E-Mail: [orders@ntis.fedworld.gov](mailto:orders@ntis.fedworld.gov)  
Online order: <http://www.ntis.gov/help/ordermethods.asp?loc=7-4-0#online>



SAND2009-7941  
Unlimited Release  
Printed December 2009

# Local Magnitudes of Small Contained Explosions

Eric P. Chael  
Ground-Based Monitoring R&E  
Sandia National Laboratories  
P.O. Box 5800  
Albuquerque, New Mexico 87185-MS0404

## Abstract

The relationship between explosive yield and seismic magnitude has been extensively studied for underground nuclear tests larger than about 1 kt. For monitoring smaller tests over local ranges (within 200 km), we need to know whether the available formulas can be extrapolated to much lower yields. Here, we review published information on amplitude decay with distance, and on the seismic magnitudes of industrial blasts and refraction explosions in the western U. S. Next we measure the magnitudes of some similar shots in the northeast. We find that local magnitudes  $M_L$  of small, contained explosions are reasonably consistent with the magnitude-yield formulas developed for nuclear tests. These results are useful for estimating the detection performance of proposed local seismic networks.

## **ACKNOWLEDGMENTS**

Tom Brocher of the USGS kindly provided his spreadsheet of data on explosions from numerous refraction experiments.

# CONTENTS

1. Introduction.....	9
2. Local magnitude scales, $M_L$ .....	11
3. Magnitude-yield relations for underground nuclear tests .....	13
4. Seismic magnitudes of sub-kiloton explosions.....	17
5. $M_L$ estimates for refraction shots in the northeastern U. S. ....	21
6. Conclusions.....	29
7. References.....	31
Distribution .....	34

# FIGURES

Figure 1. Distance correction curves ( $\log A_0(\Delta)$ ) for $M_L$ scales used by several local networks. The lower and upper dotted curves are the tabulated values of Richter (1935) and Ebel (1982), respectively. The others are based on parametric curves with spreading and attenuation terms. Each is plotted for its applicable distance range. Shown are curves from: Haines (1981), Bakun and Joyner (1984), Greenhalgh and Singh (1986), Hutton and Boore (1987), Alsaker et al. (1991), Kim (1998), Langston et al. (1998), Spallarosa et al. (2002), Shoja-Taheri et al. (2008), and Askari et al. (2009).	12
Figure 2. Plot of $m_b(Pn)$ vs. yield of NTS tests, from Vergino and Mensing (1990).	14
Figure 3. Plot of $M_L$ vs. $m_b$ for NTS tests from 1981 to 1990. Data are from the NEIC's <i>Preliminary Determination of Epicenters</i> .	16
Figure 4. Magnitude vs. yield for both chemical and nuclear explosions worldwide, from Khalturin et al. (1998). The larger events toward the upper right are mostly underground nuclear tests. The conventional explosions shown here varied from fully contained underground shots to surface blasts. The line gives the authors' suggested relation for the upper limit of magnitude as a function of yield in tons.	17
Figure 5. Magnitude vs. charge weight for chemical explosions in the western United States, from Brocher (2003).	18
Figure 6. Shot locations for the 1988 O-NYNEX refraction survey, and station BML.	21
Figure 7. Velocity response of the GS-13 sensors used at station BML (green), and the nominal Wood-Anderson velocity response (blue).	22
Figure 8. High SNR event. The top plot shows the original recorded signal from the vertical GS-13 at station BML for an explosion at a distance of 16 km. In the middle is the synthetic Wood-Anderson trace obtained from the GS-13 signal. Applying a highpass filter with a corner frequency of 0.6 Hz to the Wood-Anderson signal produces the trace at the bottom. For this	

large-amplitude signal, the filter has little apparent effect. Time is measured from the shot time of the source. 24

Figure 9. Medium SNR event at a distance of 263 km from BML. Here the highpass filter removes much of the microseismic noise seen in the middle trace, but the maximum amplitude measurement for  $M_L$  can be made with or without the filter. 25

Figure 10. Low SNR event 254 km from BML. In this case, the highpass filter is needed to enable an amplitude measurement from the Wood-Anderson signal. Note that the event is much clearer on the GS-13 record because of its higher-frequency passband compared to the Wood-Anderson. 26

Figure 11. Top: estimated  $M_L$  versus distance for the O-NYNEX explosions. The lack of a trend with distance supports Ebel's correction table for  $M_L$ . Bottom:  $M_L$  versus charge weight, plotted with Brocher's data (small black dots) on the same scales as Figure 5. The solid lines show Murphy's magnitude-yield relations for STS and NTS nuclear tests; the dashed lines have been adjusted for chemical explosives. The measurable O-NYNEX shots all used close to 1 metric ton of explosives, so the range in size is not sufficient to reveal the trend of  $M_L$  with yield. 27

## NOMENCLATURE

ANFO	ammonium nitrate/fuel oil
BML	Blue Mountain Lake
CASPAR	Close Access Sensors, Planning, and Analysis Research
IMS	International Monitoring System
NPE	Non-Proliferation Experiment
NTS	Nevada Test Site
O-NYNEX	Ontario, New York, New England Experiment
SNR	signal-to-noise ratio
STS	Semipalatinsk Test Site
USGS	United States Geological Survey
W-A	Wood-Anderson



# 1. INTRODUCTION

Sandia's Close Access Sensors, Planning, and Analysis Research (CASPAR) project was established to define and improve the capabilities of local seismic and acoustic monitoring of small explosions. Current global monitoring networks, such as the IMS, were designed to have stations within regional or teleseismic distances of most of the world's continental areas. With such station spacing, these networks can reliably detect seismic events with magnitudes above 3.0 to 3.5 worldwide, consistent with their design goals (Hafemeister, 2007). This level corresponds to well-coupled underground explosions of approximately a few hundred tons or larger. To push monitoring levels significantly below magnitude 3 or so will require stations within local distances of particular sites, that is at ranges of 200 km or less. Local networks operate in many places around the world, primarily to address seismic hazards in active zones or areas that have suffered damaging earthquakes in the past. Local-network bulletins commonly report events with magnitudes well below 2. Much is known about the operational capabilities of local networks, but some questions remain for local monitoring of explosions. The CASPAR project is intended to identify and address such questions.

The CASPAR project plan defines three research areas that can help prepare the United States to be ready to conduct effective local monitoring at desired sites. The first topic, Sensors and Systems, focuses on the required hardware capabilities for local stations. Ideally, such stations would be small, low-power, and autonomous, yet offer advanced performance and high reliability. Under CASPAR we plan to document required hardware specifications and identify commercially-available components (sensors, digitizers, processors, etc.) that meet those specs. Later, we could address system-architecture issues, which would cover all aspects of a deployable unit, including power and communications. The second research area for CASPAR is Signal Processing and Analysis. This will address effective methods for analyzing local seismic and acoustic signals in order to detect and characterize events of concern. The analysis routines should be suitable for implementation within the field system, to reduce data communication to a minimum. In FY09, we have begun this effort by exploring the range of amplitudes and frequencies to be expected from small local explosions. The third research area is Deployment Planning and Performance Estimation. We are developing software applications for modeling the performance of hypothetical deployments of local stations, similar to existing network simulation programs used for teleseismic and regional networks. For this, we will need the best available information on source scaling of small explosions, and on signal propagation within 200 km of the epicenter.

This report covers our initial work on Signal Processing and Analysis. In particular, we have researched the ground motions observed at local distances from underground explosions of 1 kg to 1 kt. This information will be important for all three CASPAR topics. Clearly, it affects the design of detection and analysis algorithms, e.g., optimal detector passbands and yield estimation relations. In addition, the results contribute to the prediction equations needed for performance estimation software (Topic 3), and they help establish hardware specifications such as dynamic range and frequency band (Topic 1).

The key question addressed in this report is whether existing magnitude-yield formulas based on regional and teleseismic signals from kiloton-to-megaton underground nuclear tests can be extrapolated to much lower yields (1 ton or even 1 kg), recorded at local ranges. We begin by reviewing published information on local magnitude ( $M_L$ ) scales. Richter's (1935) original scale for southern California has since been adapted for use in many regions around the world. For our purposes, the range of amplitude-distance decay curves that have been reported can provide bounds for the propagation parameters used for local-network modeling. Next we address published magnitude-yield relations for nuclear tests, to bound the source-scaling issue. These relations are compared to available information on magnitudes of sub-kiloton chemical explosions. Finally, we present some data from 1-ton refraction-survey explosions detonated at ranges of 15 km to 300 km from a station in northern New York.  $M_L$  estimates are determined for these shots and compared to published information on explosions of similar size, mostly in the western United States.

## 2. LOCAL MAGNITUDE SCALES, $M_L$

Richter (1935) introduced the original method of assigning magnitudes to earthquakes. His formula (since known as the ‘Richter scale’) was developed for quantifying quakes in southern California using stations at local to near-regional distances, within 600 km of the source. These are now referred to as local magnitudes, designated as  $M_L$ . To facilitate making the necessary measurements, he specified using the maximum trace amplitude from the output of a particular seismograph, the Wood-Anderson torsion instrument (Anderson and Wood, 1925). A magnitude 3 earthquake was arbitrarily defined as one which produced a maximum trace deflection of 1 mm at a distance of 100 km. Available only as horizontal sensors, the Wood-Andersons had a response function flat to ground displacement above their natural frequency of about 1.25 Hz. The subsequent development of a teleseismic body-wave magnitude scale by Gutenberg (1945) was calibrated to produce values consistent with  $M_L$  values in southern California. This scale allowed for differing sensors, by incorporating corrections for instrument gain and signal period. Gutenberg’s teleseismic scale eventually evolved into today’s  $m_b$  scale, which is the basis for the most reliable magnitude-yield relations currently available.

Though Richter recognized that his distance correction table would probably need to be modified for regions other than California, Ebel (1982) was among the first to put forward a table for an area with significantly different amplitude decay, the northeastern United States. In that geologically stable setting, seismic amplitudes exhibit less decay with distance than in tectonically active southern California. Ebel demonstrated that  $M_L$  estimates for events in the northeast based on Wood-Anderson (W-A) records and Richter’s table tended to be higher than the corresponding  $m_b$  estimates. His corrected table removed this bias, and its values converged to Richter’s with decreasing range. In other words, Ebel attempted to tie  $M_L$  values in the northeast more closely to  $m_b$ , not to Richter’s definition based on trace amplitudes at a reference distance of 100 km.

Since Ebel’s 1982 paper, many researchers around the globe have developed  $M_L$  scales appropriate for their local networks. In most cases, these are still based on Wood-Anderson amplitudes, either from actual W-A instruments or from signals recorded with other sensors, including vertical ones, then digitally converted to the effective W-A response (Bakun and Lindh, 1977). Unfortunately, a number of discrepancies have arisen among the various  $M_L$  scales. First there is the mixed application of vertical and horizontal recordings. Next, there is some uncertainty in the true gain of the W-A instruments: most assume the standard value of 2800, but Uhrhammer and Collins (1990) showed compelling evidence that the actual gains may be about 2080, and a few have adopted this value when converting signals. Probably most significant are different choices of reference among the various networks. Many have opted to connect their scales at Richter’s reference distance of 100 km, some at a distance of 17 km (using Richter’s table, an  $M_L$  3 event gives a W-A amplitude of 10 mm at 17 km), and a few have favored Ebel’s choice of calibrating their  $M_L$  scales to be consistent with  $m_b$ . Langston et al. (1998), using data from stations in Tanzania, showed that the choice of a reference can lead to  $M_L$  estimates differing by up to half a magnitude unit. Figure 1 shows distance correction curves for several published  $M_L$  scales. As expected, the curves for tectonic regions generally show more rapid decay with distance than those for stable areas. One interesting exception is the upper

blue curve for the East African Rift Zone in Tanzania (Langston et al., 1998). Propagation there seems to be quite efficient, despite the tectonic setting. When estimating the performance of local seismic networks, we can use the various curves in Figure 1 to capture the expected range in decay behavior.

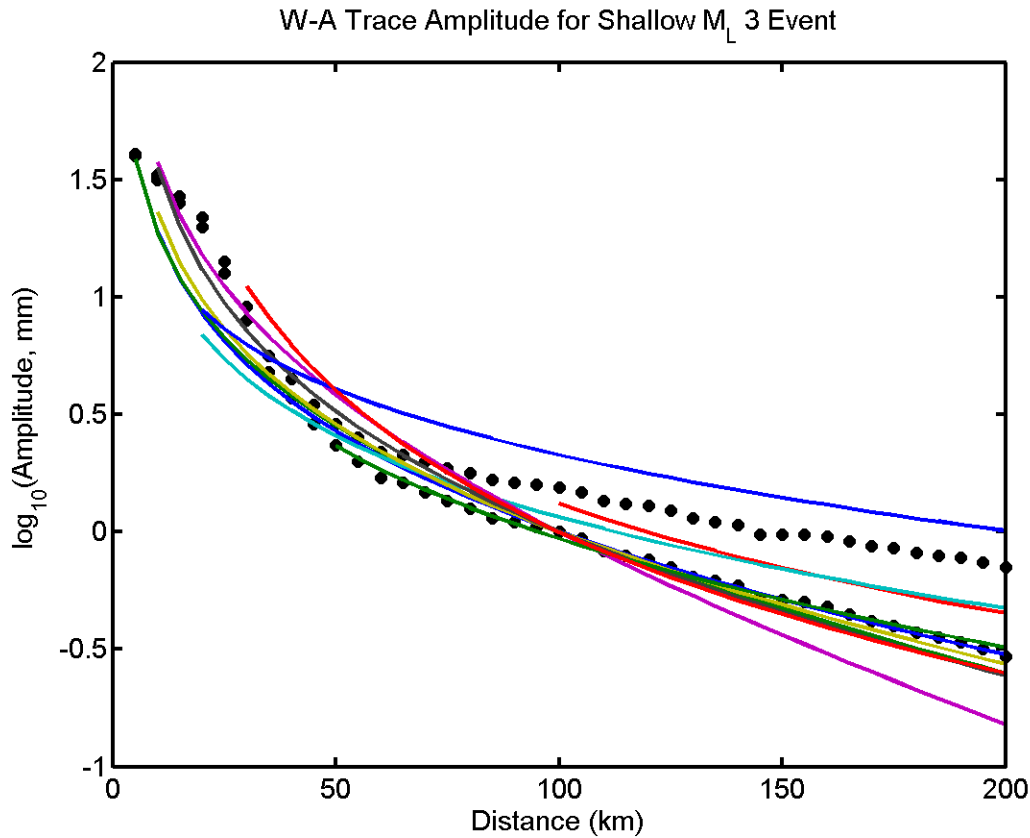


**Figure 1. Distance correction curves ( $\log A_0(\Delta)$ ) for  $M_L$  scales used by several local networks.** The lower and upper dotted curves are the tabulated values of Richter (1935) and Ebel (1982), respectively. The others are based on parametric curves with spreading and attenuation terms. Each is plotted for its applicable distance range. Shown are curves from: Haines (1981), Bakun and Joyner (1984), Greenhalgh and Singh (1986), Hutton and Boore (1987), Alsaker et al. (1991), Kim (1998), Langston et al. (1998), Spallarosa et al. (2002), Shoja-Taheri et al. (2008), and Askari et al. (2009).

### 3. MAGNITUDE-YIELD RELATIONS FOR UNDERGROUND NUCLEAR TESTS

Yield estimates for underground nuclear tests are generally obtained from their seismic magnitudes and an empirical magnitude-yield relationship. For most test sites, the preferred choice is the classic teleseismic  $m_b$  and a relation of the form:

$$m_b = A + B \cdot \log(Y)$$

for yield  $Y$  in kilotons. Calibration of this equation for the constants  $A$  and  $B$  has primarily relied on tests with yields of one to several hundred kilotons. The most extensive calibration data are available for the Nevada Test Site (NTS); the Department of Energy has released independent yield values for many of the tests there. For NTS, Murphy (1981) proposed the formula:

$$m_b = 3.92 + 0.81 \cdot \log(Y, \text{ kt})$$

for shots in hard rock or below the water table. He reported that tests in dry alluvium at NTS could have magnitudes as much as 1 unit lower. Vergino and Mensing (1990) used  $m_b$  values derived from regional  $P_n$  amplitudes to obtain the relation:

$$m_b(P_n) = A_R + 0.91 \cdot \log(Y, \text{ kt})$$

with an intercept  $A_R$  that varies between 3.76 and 3.87 for different areas within NTS. They showed that a single correction for the gas-filled porosity at the shot location led to consistent results among tests in any type of rock at NTS, including dry alluvium. Figure 2 displays their magnitude and yield data, with this correction applied.

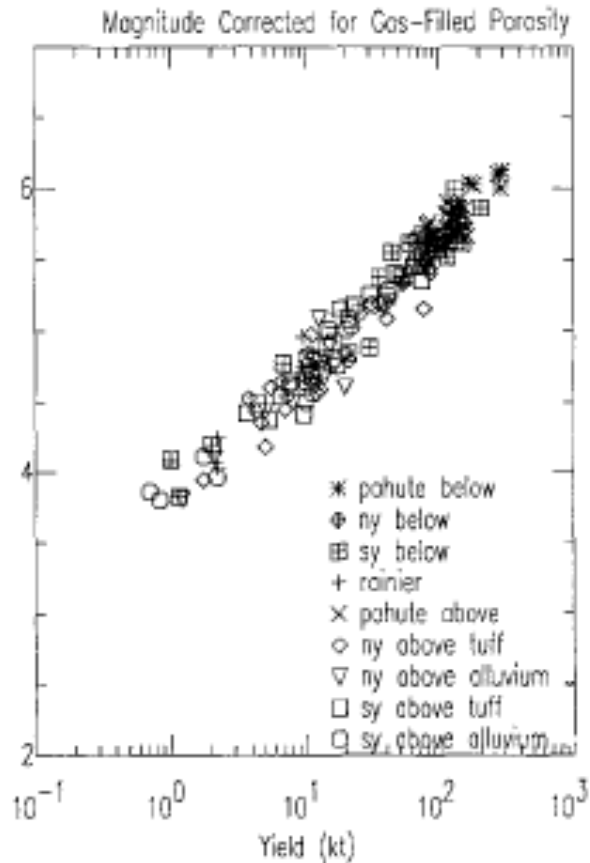


**Figure 2. Plot of  $m_b(P_n)$  vs. yield of NTS tests, from Vergino and Mensing (1990).**

There is general agreement that the tectonic setting of NTS leads to some reduction in the seismic magnitude resulting from a test of a given yield, thought to be due to upper-mantle attenuation beneath the site. Thus, tests at sites in stable continental areas are expected to produce somewhat higher magnitudes than seen from the same yield at NTS. Unfortunately, relatively few independent yield values are available for sites other than NTS. Murphy (1996) determined the magnitude-yield relation for the Soviet Union's Semipalatinsk Test Site (STS) to be:

$$m_b = 4.45 + 0.75 \cdot \log(Y, \text{ kt})$$

based on the observed spectra of teleseismic P waves from the Soviet tests, and relative estimates of the attenuation parameter  $t^*$  for the western U. S. and central Asia. Russian scientists have published yield values for a handful of the Soviet tests that agree extremely well with this formula for STS (Bocharov et al., 1989), but some of the released yields may themselves have been derived from seismic measurements. Though certainly not as well calibrated as the NTS formulas, Murphy's STS formula remains the most widely accepted magnitude-yield relation for

that site currently available in the open literature. It produces  $m_b$  values for Semipalatinsk tests that are approximately 0.5 magnitude units larger than those from NTS shots at the same yield.

Two questions must be addressed before we can confidently use the equations above to predict the magnitudes expected from the small explosions which motivate the use of local monitoring stations. First, nearly all published magnitude-yield formulas, including those above, are based on nuclear tests in the yield range of 1 kt to 1 Mt, and there is no guarantee that they can be extrapolated far outside this range, to yields as low as 1 ton or even below. In the following sections, we examine this extrapolation by considering the available evidence from chemical explosions below 1 kt. The second issue concerns the transition in magnitude scales from teleseismic  $m_b$ , which is readily measured for tests larger than 1 kt, to a local scale such as  $M_L$ , which will be the only type available for small events observable only within a few hundred kilometers of the source. As mentioned above, the  $m_b$  scale was developed to be consistent with Richter's local magnitudes for southern California. Figure 3 compares  $m_b$  and  $M_L$  measurements for NTS tests from 1981 to 1990. The agreement between the scales demonstrated in this figure indicates that we can substitute  $M_L$  for  $m_b$  in a magnitude-yield relation for the California-Nevada region. Such a substitution may be problematic in other areas, particularly where the  $M_L$  scale is tied to Richter's definition at 100 km and not to the  $m_b$  values of larger events in the area (refer to the preceding section). In such places, there may be some consistent bias between  $m_b$  and  $M_L$  estimates.

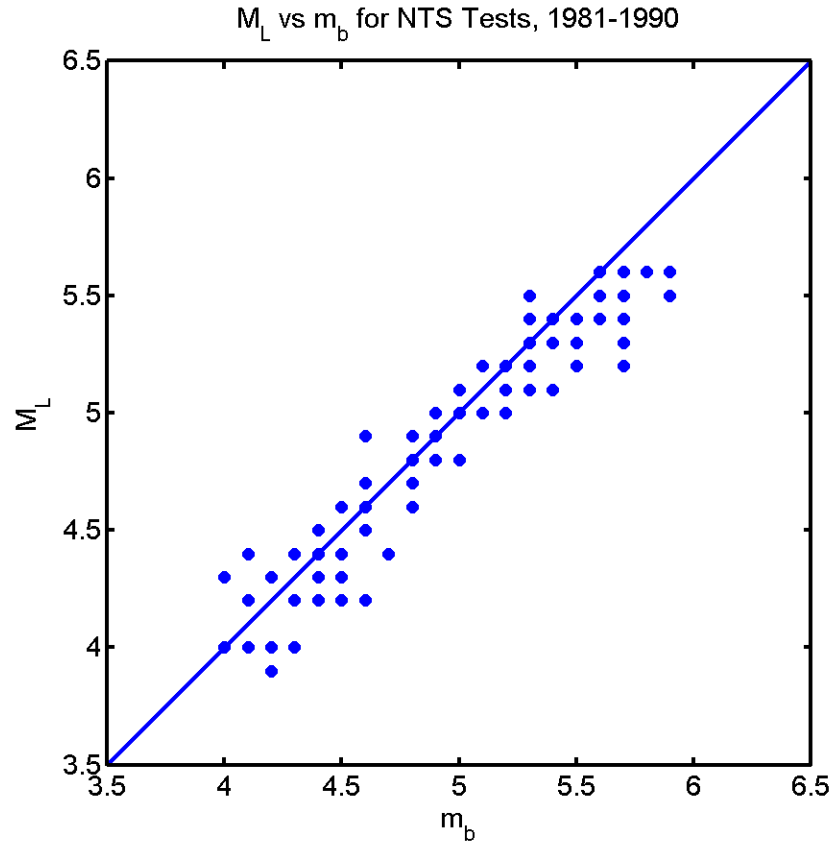


**Figure 3. Plot of  $M_L$  vs.  $m_b$  for NTS tests from 1981 to 1990.** Data are from the NEIC's *Preliminary Determination of Epicenters*.

#### 4. SEISMIC MAGNITUDES OF SUB-KILOTON EXPLOSIONS

Compared to the available literature on magnitude-yield relations for underground nuclear tests, relatively little has been published on seismic magnitudes for chemical explosions of much lower yield. Most of what is available focuses on the issue of screening from a monitoring network's bulletin the large numbers of chemical explosions detonated by mining, quarrying, and construction firms. For this purpose, the reliability of any yield formula is of secondary concern. Khalturin et al. (1998) presented yield and magnitude information for many mining blasts between 1 and 1000 tons. Figure 4 reproduces a plot from their paper which compares such events to data for nuclear tests and some large research explosions.

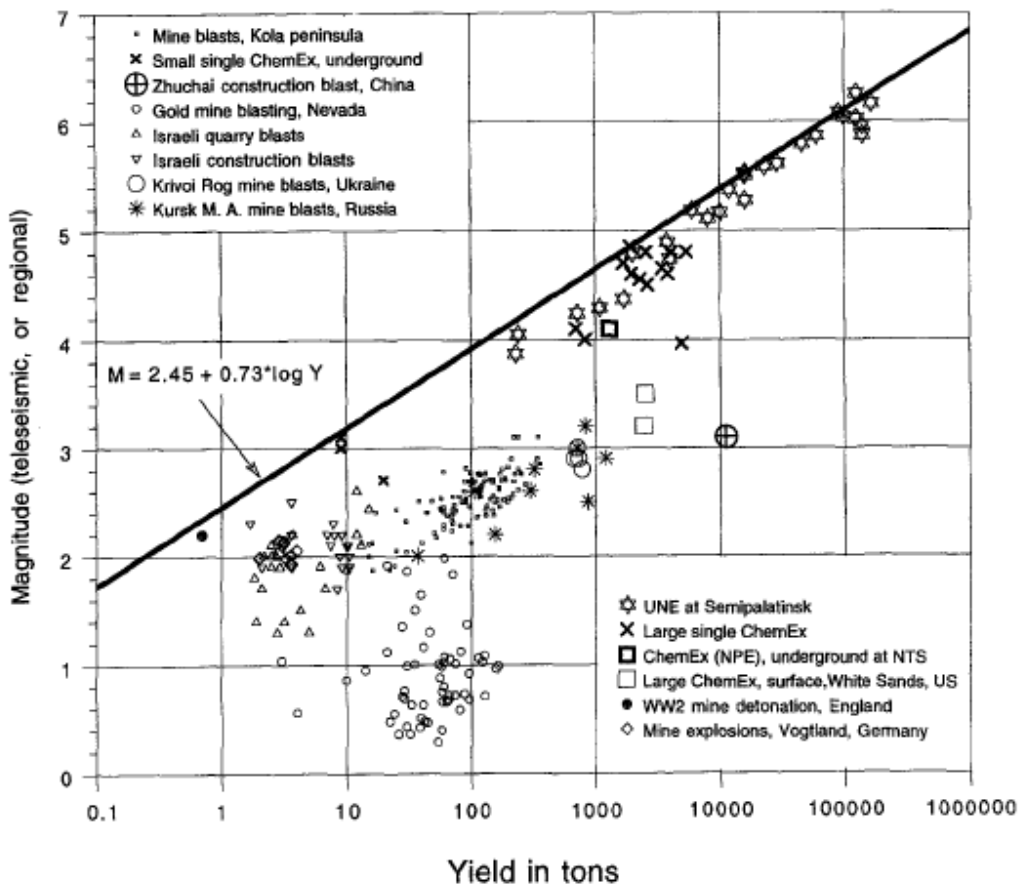


**Figure 4. Magnitude vs. yield for both chemical and nuclear explosions worldwide, from Khalturin et al. (1998).** The larger events toward the upper right are mostly underground nuclear tests. The conventional explosions shown here varied from fully contained underground shots to surface blasts. The line gives the authors' suggested relation for the upper limit of magnitude as a function of yield in tons.

On first inspection, this plot suggests that the magnitude-yield trend for the nuclear tests is not appropriate for smaller chemical explosions. However, a large majority of the mine blasts used for this figure were conducted at the surface, so they were decoupled to some degree in comparison with the tamped and contained nuclear tests. The chemical shots on the plot which fall closer to the trend of the nuclear ones tend to represent better-contained blasts deeper underground. Note that for the purposes of screening, the tendency of most of the large chemical shots to give smaller magnitudes is beneficial, since they become less likely to be detected by a global monitoring network.

A more recent compilation of data from chemical explosions in the western United States was published by Brocher (2003). His data are displayed in Figure 5.

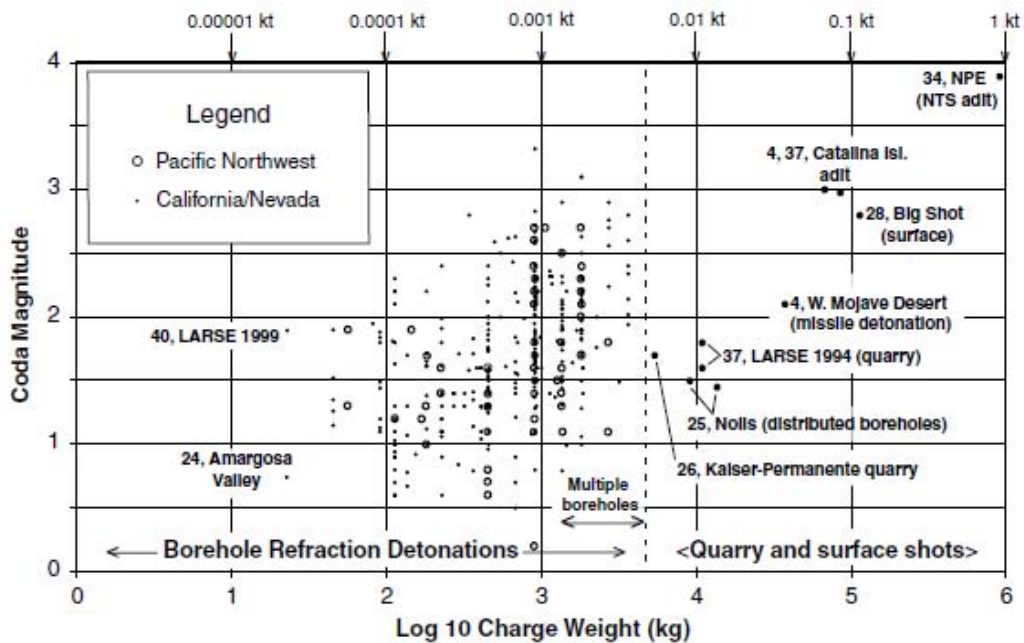


**Figure 5. Magnitude vs. charge weight for chemical explosions in the western United States, from Brocher (2003).**

Brocher includes a few surface detonations, most at yields above 10 tons. The bulk of his data, though, are from tamped, single-charge explosions, primarily USGS refraction shots of 1/10 to a few tons. Most of the magnitude estimates were derived from coda duration measurements at local stations; such coda scales are typically intended to approximate genuine  $M_L$  values. These events display substantial scatter in their reported magnitudes. This scatter has several possible causes, including variations in emplacement medium, in the type of explosive used and its method of loading, and in the completeness of combustion. Murphy's magnitude-yield formulas for NTS and STS predict magnitudes of 1.5 and 2.2, respectively, for a 1-ton nuclear test. Both values fall within the cloud of points near the center of Figure 5. Given the scatter in these data, either formula seems equally valid. The nearly 1 kt chemical explosion of the Non-Proliferation

Experiment (NPE; Denny et al., 1996) at NTS appears at the upper right of the plot. This particular sample falls very close to Murphy's NTS relation, which gives a magnitude of 3.9 for a 1-kt source. Below, we will further discuss the comparison between chemical explosions and the nuclear magnitude-yield relations.



## 5. $M_L$ ESTIMATES FOR REFRACTION SHOTS IN THE NORTHEASTERN U. S.

Nearly all of the chemical explosion magnitudes reported by Brocher (2003; Fig. 5) were measured for shots in the far western United States. Similar data for explosions in stable central or eastern North America seem to be less readily available. We present here some  $M_L$  estimates for a series of contained, single-borehole explosions in the northeast that were conducted as part of a refraction survey in 1988. The U. S. Geological Survey, the Air Force Geophysics Laboratory, and the Geological Survey of Canada performed this experiment to study the structure from Maine to Ontario, across the Adirondacks and Appalachians and onto the Canadian Shield. Details of the survey, including shot locations, times, and charge weights, are available in a USGS Open File Report (Luetgert et al., 1990). Sandia Labs and Rondout Associates, Inc. recorded these explosions using high-gain, high-frequency instrumentation as part of a study to determine the utility of frequencies above 20 Hz for regional monitoring of nuclear testing (Barstow et al., 1990; Chael et al., 1995). Figure 6 shows the shot locations and the site of the Sandia/Rondout station near Blue Mountain Lake, New York (BML). The epicentral distances to BML ranged from 15 to 390 km. Most of the shots used between 900 and 1300 kg of ANFO, while the smallest used 270 kg and the largest 2090 kg.

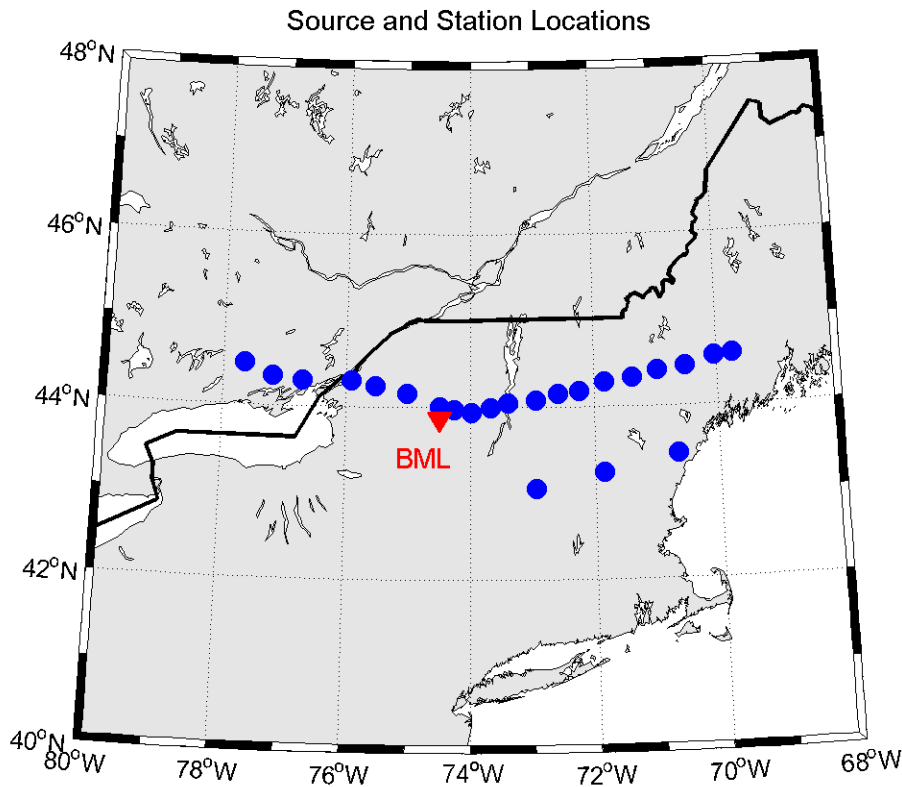
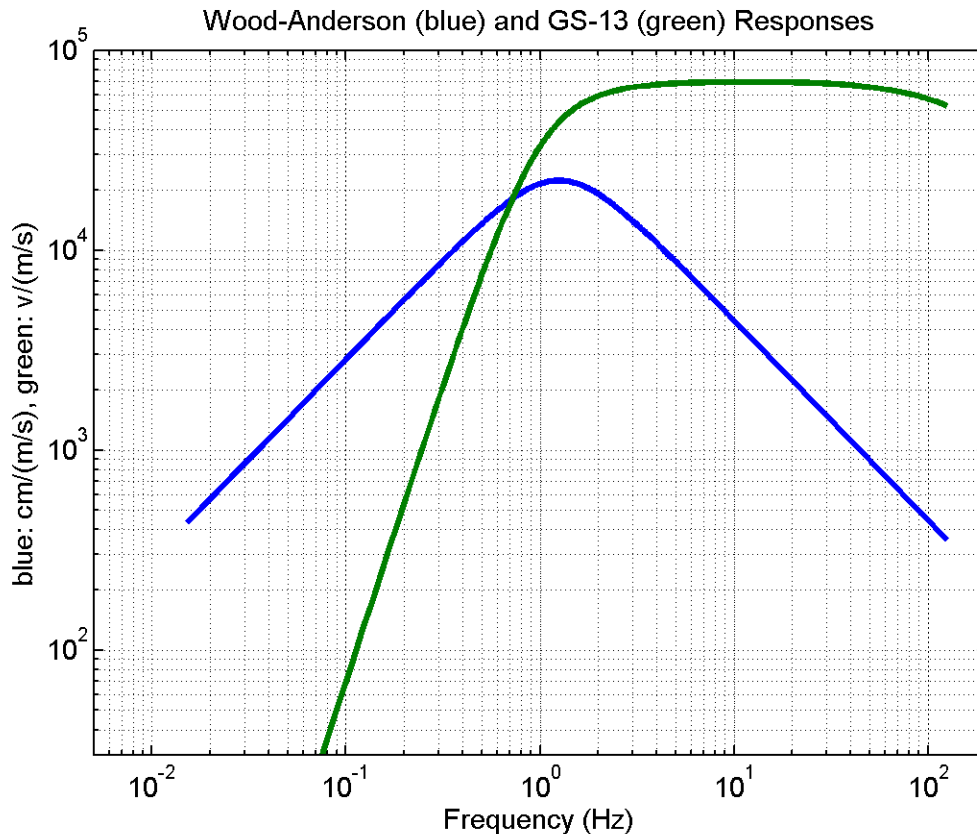


Figure 6. Shot locations for the 1988 O-NYNEX refraction survey, and station BML.

The station at BML consisted of a three-component set of Geotech GS-13 seismometers, Geotech DHL-70 preamplifiers, and a RefTek 72-02 16-bit data acquisition system. Signals from the explosions were recorded at either 200 or 250 sps, at two different gains on the RefTek. The higher gain allowed adequate resolution of the low background noise at the site, while the lower gain recorded the closest explosions without clipping. The velocity response of the BML seismic system is relatively flat over the frequency band of 2-100 Hz. Figure 7 compares the velocity response of the BML sensor and amplifier combination with that of the nominal Wood-Anderson seismometer ( $T_0 = 0.8$  s, damping = 0.8, gain = 2800). Note that the output units of these sensors differ (volts vs. centimeters), so a direct comparison of the curves is valid for the relative response shapes, but not the relative levels. The Wood-Anderson is actually flat to ground displacement above its natural frequency of 1.25 Hz, so its output should approximately resemble the time-integrated signal from a GS-13.



**Figure 7. Velocity response of the GS-13 sensors used at station BML (green), and the nominal Wood-Anderson velocity response (blue).**

To estimate  $M_L$  magnitudes for the explosions, we first converted the recorded vertical signals to ‘synthetic W-A’ traces by deconvolving the GS-13 response and then convolving the result with that of a Wood-Anderson (Bakun and Lindh, 1977). Figures 8 to 10 show three samples of the recorded and converted seismograms. The third trace at the bottom of each figure results from

applying a highpass Butterworth filter with a corner frequency of 0.6 Hz to the W-A signals in the middle. This filter significantly reduces the lower-frequency microseismic background, but has relatively little effect on the overall character, or the peak amplitude, of the P and S arrivals from the explosions. Figure 8 plots the traces for one of the closer shots to BML, one with a very high signal-to-noise ratio (SNR). In this case, the arriving signal is well above the background on all three signals, and W-A peak amplitudes are essentially identical whether measured with or without the highpass filter (i.e., from the third or second traces). The more distant shot displayed in Figure 9 has lower overall signal-to-noise. As a result, the conversion to a synthetic W-A signal (Fig. 9, middle) results in P and S arrivals whose amplitudes are not much above the level of the microseisms. The highpass filter (Fig. 9, bottom) enhances the P and S arrivals here, but even for this borderline case the peak W-A signal amplitude can be measured with or without the filter. Figure 10 demonstrates what happens with an even weaker signal. This time the explosion signal is almost completely lost in the background noise in the middle trace, and the filter is necessary here to bring the signal out from the noise so that one can measure the peak amplitude. For a few of the most distant shots, even the highpass filter could not enable a W-A amplitude measurement to be made, despite the fact that most of these had reasonably clear and measurable arrivals on the original GS-13 traces. The improved high-frequency response of modern electromagnetic sensors like the GS-13, and their steeper roll-off at low frequencies, make them better suited for observing small local and near-regional events than displacement instruments like the Wood-Anderson.

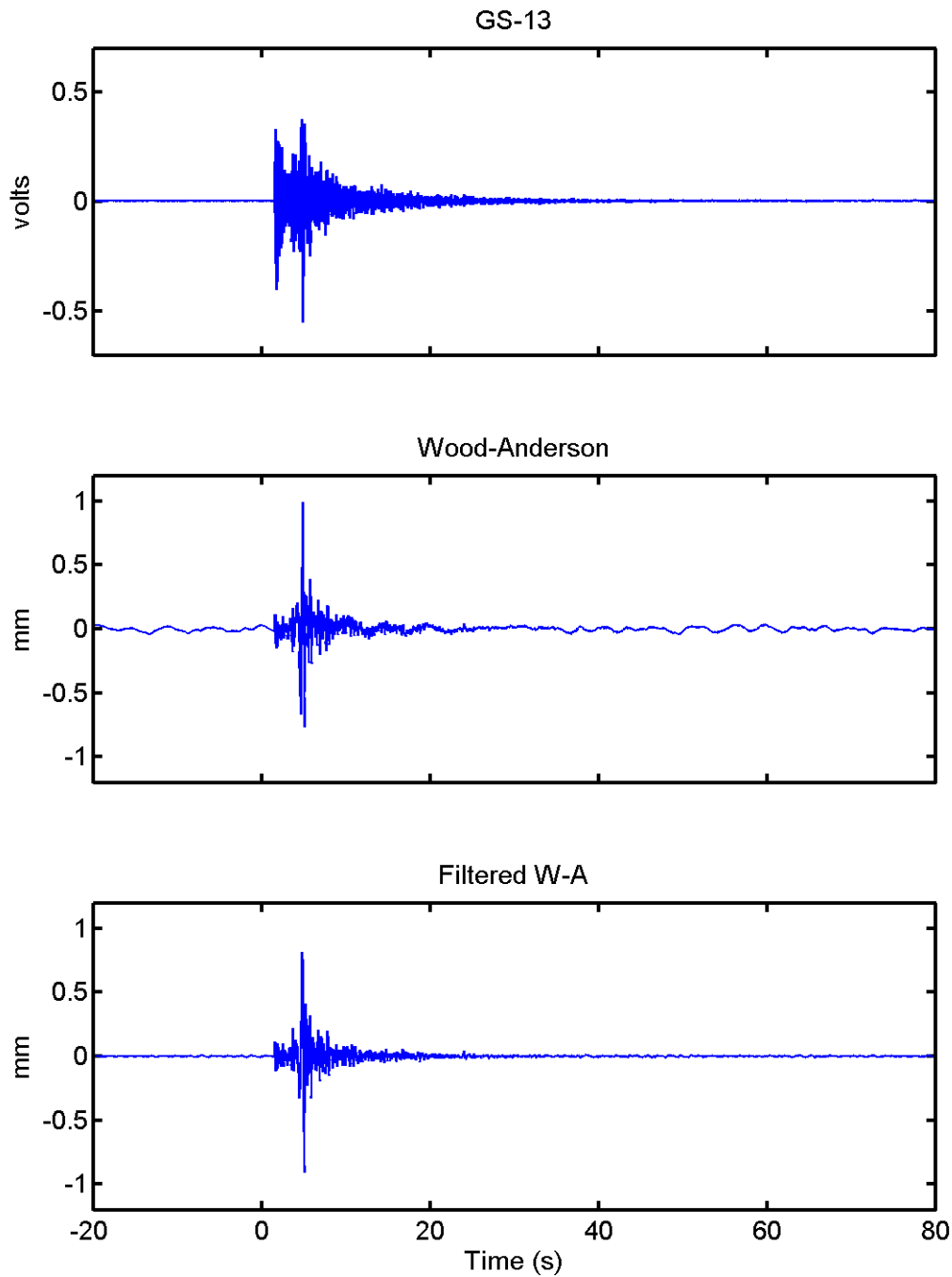


**Figure 8. High SNR event.** The top plot shows the original recorded signal from the vertical GS-13 at station BML for an explosion at a distance of 16 km. In the middle is the synthetic Wood-Anderson trace obtained from the GS-13 signal. Applying a highpass filter with a corner frequency of 0.6 Hz to the Wood-Anderson signal produces the trace at the bottom. For this large-amplitude signal, the filter has little apparent effect. Time is measured from the shot time of the source.

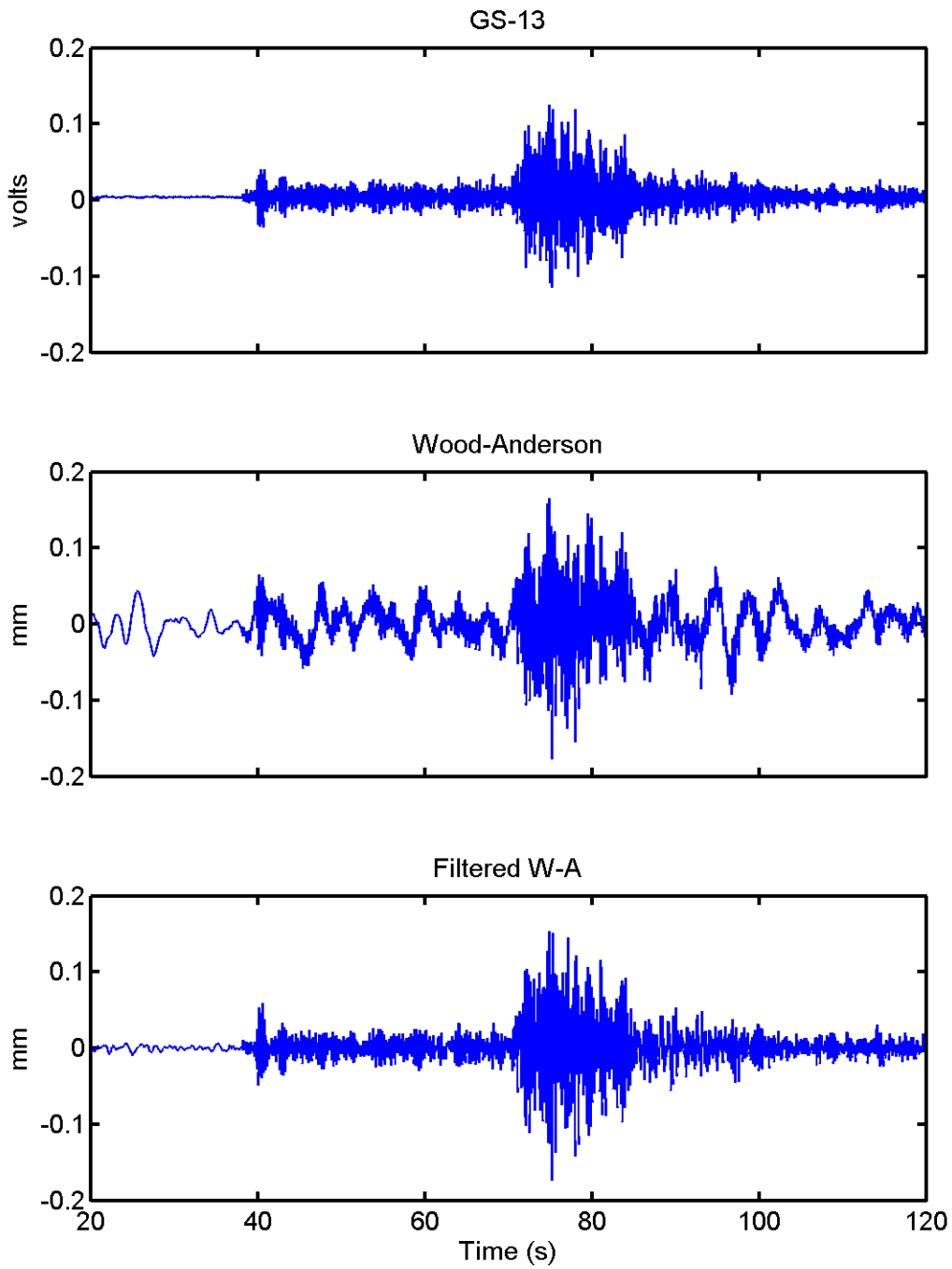


**Figure 9. Medium SNR event at a distance of 263 km from BML.** Here the highpass filter removes much of the microseismic noise seen in the middle trace, but the maximum amplitude measurement for  $M_L$  can be made with or without the filter.

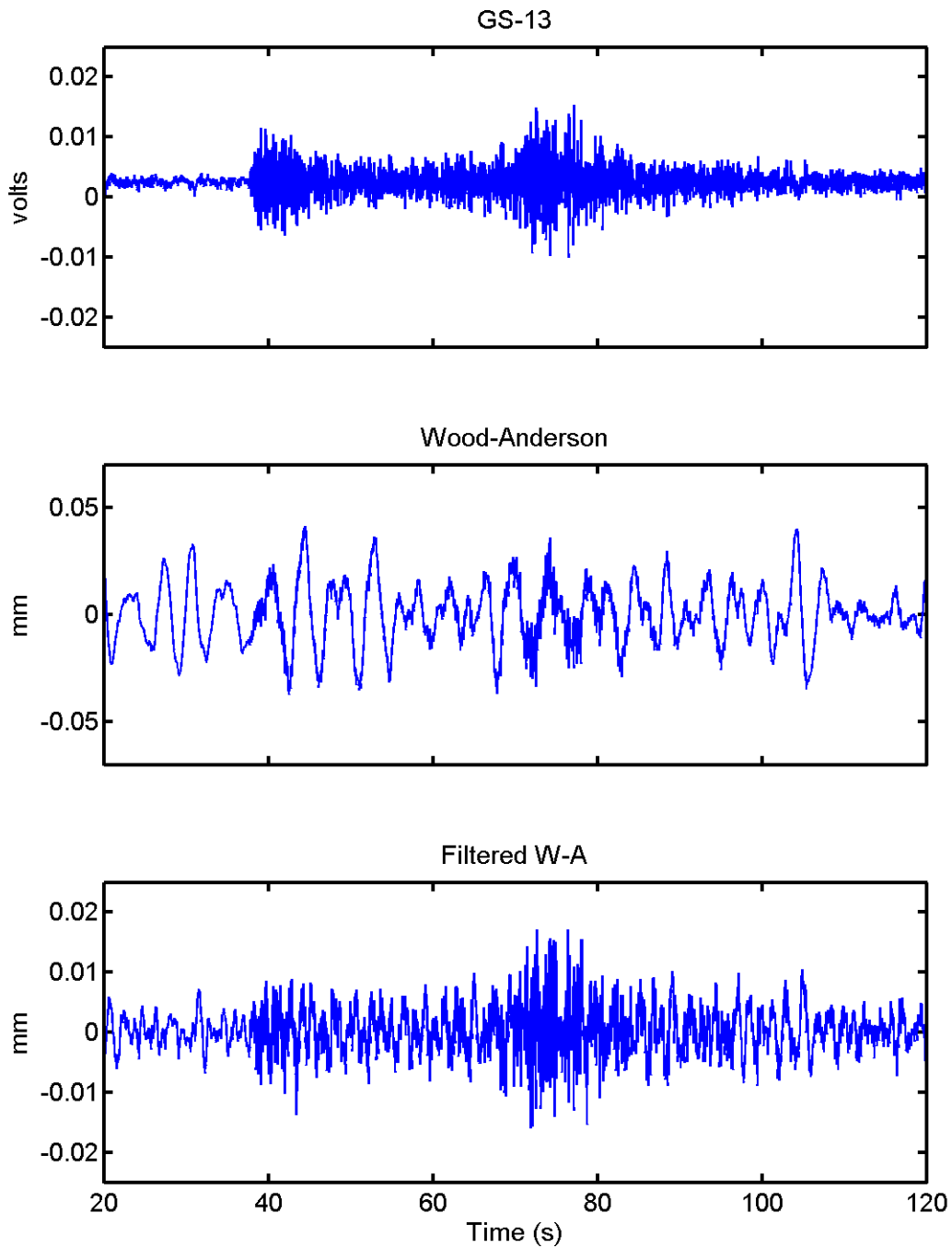


**Figure 10. Low SNR event 254 km from BML.** In this case, the highpass filter is needed to enable an amplitude measurement from the Wood-Anderson signal. Note that the event is much clearer on the GS-13 record because of its higher-frequency passband compared to the Wood-Anderson.

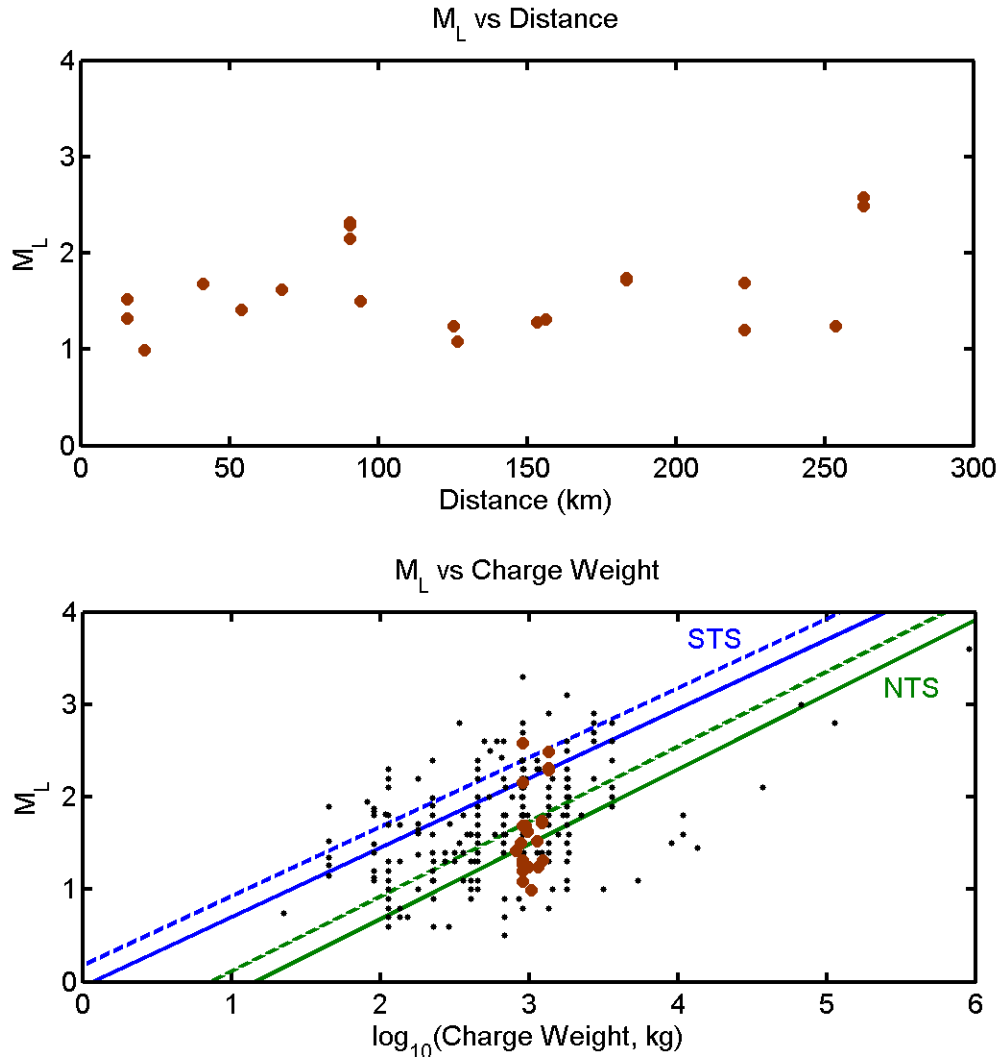


**Figure 11. Top: estimated  $M_L$  versus distance for the O-NYNEX explosions.** The lack of a trend with distance supports Ebel's correction table for  $M_L$ . **Bottom:**  $M_L$  versus charge weight, plotted with Brocher's data (small black dots) on the same scales as Figure 5. The solid lines show Murphy's magnitude-yield relations for STS and NTS nuclear tests; the dashed lines have been adjusted for chemical explosives. The measurable O-NYNEX shots all used close to 1 metric ton of explosives, so the range in size is not sufficient to reveal the trend of  $M_L$  with yield.

We applied Ebel's (1982)  $M_L$  scale for the northeastern United States to determine magnitudes for the refraction explosions. We used half the maximum peak-to-peak trace amplitude from the synthetic W-A traces; the highpass filter was used only for cases like Figure 10, where the measurement could not otherwise be made. The top of Figure 11 plots the  $M_L$  estimates against epicentral distance. The measurable shots all used close to 1 ton of ANFO. The fact that the  $M_L$  values show no residual trend with distance supports Ebel's decay curve for the northeast. The two most distant shots were fired about 200 m underwater in a quarry, which explains their

increased magnitudes. The two at a distance near 90 km and with  $M_L$  above 2 occurred close to but not in Lake Champlain. It would be interesting to know if they were fired in saturated sediments, which could explain their enhanced amplitudes. At the bottom of Figure 11, the same  $M_L$  estimates are plotted against charge weight, together with the data from Brocher (2003). The general agreement indicates that small explosions in the eastern and western United States, when measured with  $M_L$  scales appropriate for their location, give consistent local magnitudes at comparable yields. It is interesting that the shots in the east do not tend to produce higher magnitudes, as might be expected based on a comparison of the NTS and STS magnitude-yield formulas (shown as solid lines across the plot). On the other hand, the significant scatter in the data, and the very small number of available samples for the eastern U. S., may be obscuring whatever differences do exist.

There is some evidence, and a widespread belief, that the seismic efficiency of a given weight of chemical explosives is about twice that of a nuclear blast with the equivalent yield (see e.g. Denny et al., 1996). Apparently, this applies to chemical explosives similar to TNT; an equal weight of ANFO, which is commonly used for large blasts, releases somewhat less energy and thus may generate lower amplitudes than TNT. Higher-energy explosive compounds like C4, more typical for military use, might be expected to produce larger amplitudes. In any case, if one accepts the general factor-of-two difference between nuclear and chemical efficiencies, then the nuclear magnitude-yield relations are shifted as shown by the dashed lines in Figure 11. After this adjustment, Brocher's data tend to favor the NTS equation, and the one for STS falls toward the upper end of the sample distribution. Most of the events larger than several tons were quarry blasts, which produce lower magnitudes because they are not fully contained underground.

## 6. CONCLUSIONS

In order to predict the performance of a proposed local seismic network for monitoring small explosions, one needs information both on the signal decay (combined spreading, attenuation, and scattering effects) over local ranges, and on the seismic source strength of explosions with yields well below 1 kt. Published decay curves for  $M_L$  scales employed in different regions provide estimates for the former (Fig. 1). It would be preferable to know something about the frequency dependence of the decay rates for individual local arrivals, but currently such detailed information on propagation is unavailable in most areas. The  $M_L$  calibrations provide information on expected peak amplitudes for frequencies in the vicinity of 1-2 Hz, near the response peak of a Wood-Anderson seismometer. Generally this peak amplitude occurs in the S or Lg arrival, but may occur during P or Rg for some events. Despite these limitations, the  $M_L$  decay curves can still be used for an estimate of the minimum detectable magnitude at a specified distance from a station, if combined with a value for the typical ambient noise amplitude at the site. These threshold estimates will be conservative ones for local and near regional distances because they correspond to frequencies near 1 Hz, and the peak signal-to-noise at such ranges will often occur at significantly higher frequencies.

The best available evidence on the local magnitudes of small contained explosions has been presented by Brocher (2003). His data, almost entirely from the western U. S., represent chemical explosions between 1 kg and 1 kt, with most in the range of 0.1 to 10 tons. There is considerable scatter in the magnitudes at any yield, but overall the data are reasonably consistent with the magnitude-yield relations developed for nuclear explosions above 1 kt. If these relations are adjusted to account for the accepted relative seismic efficiencies of chemical and nuclear explosions, then they favor magnitude-yield formulas derived for NTS over those appropriate for low-attenuation areas like Semipalatinsk (Fig. 11). Our  $M_L$  estimates for a small number of refraction shots in the northeastern U. S. fall within the scatter of Brocher's samples. One might have expected explosions there to give somewhat larger magnitudes, closer to the  $m_b(Y)$  relation for STS, because of the low attenuation in the region. Magnitudes and yields for many more contained explosions, recorded by numerous stations, will be needed to investigate whether there are resolvable offsets in the  $M_L$  values of small shots from different regions. The local P and S signals have not traversed the upper mantle beneath the source as teleseismic arrivals do, so perhaps the  $m_b$  bias between NTS and STS will not be reflected in local magnitudes.

Discrepancies in the choice of reference used for  $M_L$  calibrations in different regions can be expected to cause some variation in the reported local magnitudes for explosions of the same size. The most common reference uses the amplitude at a distance of 100 km. However, there may be significant differences between regions in the amplitude decay from 0 to 100 km. Recognizing this, some researchers (Ebel, 1982; Hutton and Boore, 1987; Langston et al., 1998) have argued for using either a smaller epicentral distance or a calibration against  $m_b$  as the reference, so that  $M_L$  values for events in different regions will more closely represent relative source strengths.

This inconsistency among available  $M_L$  scales, and the fact that small local events usually have their best signal-to-noise at frequencies well above the band used for  $M_L$  amplitude

measurements, both suggest that an alternative to classic  $M_L$  magnitudes would be desirable for characterizing small explosions. In fact, for local test site monitoring, it may be preferable to forego magnitudes altogether, and instead directly estimate the equivalent tamped yield of an event. Kohler and Fuis (1992) published prediction equations for seismic amplitudes from small explosions, based primarily on USGS refraction profiles in the western U. S. Their equations circumvent both of the issues encountered using  $M_L$ : they are based directly on charge size instead of magnitude, and they predict peak ground velocities in the 2-100 Hz band, which should capture the peak SNR of small local events. Though the equations give only a single maximum amplitude for this wide band, they should be better for predicting the yield threshold of a local network. For reliable use outside the western U. S., however, similar equations will need to be calibrated in other areas. In the meantime, one might employ these equations with suitable spreading and attenuation coefficients for other areas, based either on available parametric  $M_L$  decay curves or regional attenuation studies of individual phases.

## 7. REFERENCES

- Alsaker, A., L. B. Kvamme, R. A. Hansen, A. Dahle, and H. Bungum (1991). The  $M_L$  scale in Norway, *Bull. Seism. Soc. Am.* **81**, 379-398.
- Anderson, J. A., and H. O. Wood (1925). Description and theory of the torsion seismometer, *Bull. Seism. Soc. Am.* **15**, 1-72.
- Askari, R., A. Ghods, and F. Sobouti (2009). Calibration of an  $M_L$  scale in the Alborz region, northern Iran, *Bull. Seism. Soc. Am.* **99**, 268-276.
- Bakun, W. H., and W. B. Joyner (1984). The  $M_L$  scale in central California, *Bull. Seism. Soc. Am.* **74**, 1827-1843.
- Bakun, W. H., and A. G. Lindh (1977). Local magnitudes, seismic moments, and coda durations for earthquakes near Oroville, California, *Bull. Seism. Soc. Am.* **67**, 615-629.
- Barstow, N., J. A. Carter, P. W. Pomeroy, G. H. Sutton, E. P. Chael, and P. J. Leahy (1990). High-frequency (1-100 Hz) noise and signal recorded at different depths in a mine, northwest Adirondacks, NY, *Geophys. Res. Lett.* **17**, 681-684.
- Bocharov, V. S., S. A. Zelentsov, and V. N. Mikhailov (1989). Characteristics of 96 underground nuclear explosions at the Semipalatinsk Test Site, *Atomnaya Energiya* **67**, 3.
- Brocher, T. M. (2003). Detonation charge size versus coda magnitude relations in California and Nevada, *Bull. Seism. Soc. Am.* **93**, 2089-2105.
- Chael, E. P., P. J. Leahy, J. A. Carter, N. Barstow, and P. W. Pomeroy (1995). Propagation of high frequency (4 to 50 Hz) P waves in the northeastern United States, *Bull. Seism. Soc. Am.* **85**, 1244-1248.
- Denny, M., P. Goldstein, K. Mayeda, and W. Walter (1996). Seismic results from DOE's Non-Proliferation Experiment: a comparison of chemical and nuclear explosions, in *Monitoring a Comprehensive Test Ban Treaty*, E. S. Husebye and A. M. Dainty (editors), 355-364.
- Ebel, J. E. (1982).  $M_L$  measurements for northeastern United States earthquakes, *Bull. Seism. Soc. Am.* **72**, 1367-1378.
- Greenhalgh, S. A., and R. Singh (1986). A revised magnitude scale for South Australian earthquakes, *Bull. Seism. Soc. Am.* **76**, 757-769.
- Gutenberg, B. (1945). Amplitudes of P, PP, and S and magnitude of shallow earthquakes, *Bull. Seism. Soc. Am.* **35**, 57-69.

- Hafemeister, D. (2007). Progress in CTBT monitoring since its 1999 Senate defeat, *Science and Global Security* **15**, 151-183.
- Haines, A. J. (1981). A local magnitude scale for New Zealand earthquakes, *Bull. Seism. Soc. Am.* **71**, 275-294.
- Hutton, L. K., and D. M. Boore (1987). The  $M_L$  scale in southern California, *Bull. Seism. Soc. Am.* **77**, 2074-2094.
- Khalturin, V. I., T. G. Rautian, and P. G. Richards (1998). The seismic signal strength of chemical explosions, *Bull. Seism. Soc. Am.* **88**, 1511-1524.
- Kim, W.-Y. (1998). The  $M_L$  scale in eastern North America, *Bull. Seism. Soc. Am.* **88**, 935-951.
- Kohler, W. M., and G. S. Fuis (1992). Empirical dependence of seismic ground velocity on the weight of explosives, shotpoint site condition, and recording distance for seismic-refraction data, *Bull. Seism. Soc. Am.* **82**, 2032-2044.
- Langston, C. A., R. Brazier, A. A. Nyblade, and T. J. Owens (1998). Local magnitude scale and seismicity rate for Tanzania, East Africa, *Bull. Seism. Soc. Am.* **88**, 712-721.
- Luetgert, J., S. Hughes, J. Cipar, S. Mangino, D. Forsyth, and I. Asudeh (1990). Data report for O-NYNEX, the 1988 Grenville-Appalachian seismic refraction experiment in Ontario, New York and New England, *U. S. Geol. Survey Open-File Rept. 90-426*, 53 pp.
- Murphy, J. R. (1981). P wave coupling of underground explosions in various geologic media, in *Identification of Seismic Sources – Earthquake or Underground Explosion*, E. S. Husebye and S. Mykkeltveit (editors), 201-205.
- Murphy, J. R. (1996). Types of seismic events and their source descriptions, in *Monitoring a Comprehensive Test Ban Treaty*, E. S. Husebye and A. M. Dainty (editors), 225-245.
- Richter, C. F. (1935). An instrumental earthquake magnitude scale, *Bull. Seism. Soc. Am.* **25**, 1-32.
- Shoja-Taheri, J., S. Naserieh, and A. H. Ghafoorian-Nasab (2008). An  $M_L$  scale in northeastern Iran, *Bull. Seism. Soc. Am.* **98**, 1975-1982.
- Spallarosa, D., D. Bindi, P. Augliera, and M. Cattaneo (2002). An  $M_L$  scale in northwestern Italy, *Bull. Seism. Soc. Am.* **92**, 2205-2216.
- Uhrhammer, R. A., and E. R. Collins (1990). Synthesis of Wood-Anderson seismograms from broadband digital records, *Bull. Seism. Soc. Am.* **80**, 702-716.
- Vergino, E. S., and R. W. Mensing (1990). Yield estimation using regional  $m_b(Pn)$ , *Bull. Seism. Soc. Am.* **80**, 656-674.

## DISTRIBUTION

- 1 Randy Bell  
NNSA Office of Nonproliferation Research and Development/NA-22  
1000 Independence Avenue SW  
Washington, DC 20585
- 1 Leslie Casey  
NNSA Office of Nonproliferation Research and Development/NA-22  
1000 Independence Avenue SW  
Washington, DC 20585
- 1 John Ziagos  
NNSA Office of Nonproliferation Research and Development/NA-22  
1000 Independence Avenue SW  
Washington, DC 20585
- 1 John Dwyer  
Air Force Technical Applications Center/TTR  
1030 S. Highway A1A  
Patrick AFB, FL 32925-3002
- 1 Mark Woods  
Air Force Technical Applications Center/TTR  
1030 S. Highway A1A  
Patrick AFB, FL 32925-3002
- 1 Bill Walter  
Lawrence Livermore National Laboratory  
MS L-046  
PO Box 808  
Livermore, CA 94551
- 1 Ward Hawkins  
Los Alamos National Laboratory  
MS F665  
PO Box 1663  
Los Alamos, NM 87545
- 1 Thomas Brocher  
U. S. Geological Survey, MS/977  
345 Middlefield Ave.  
Menlo Park, CA 94025

1	MS0401	Dorthe Carr	5527
1	MS0401	Ben Hamlet	5527
1	MS0401	Chris Young	5527
1	MS0404	Eric Chael	5736
1	MS0404	Bobby Corbell	5736
1	MS0404	Darren Hart	5736
1	MS0404	Tim McDonald	5736
1	MS0404	John Merchant	5736
1	MS0404	Randy Rembold	5736
1	MS0404	Megan Resor	5736
1	MS0899	Technical Library	9536 (electronic copy)



**Sandia National Laboratories**